Biosensors and Bioelectronics 26 (2010) 736–742

Contents lists available at ScienceDirect

Biosensors and Bioelectronics

journal homepage: www.elsevier.com/locate/bios

Electrochemical detection of D-dimer as deep vein thrombosis marker using single-chain D-dimer antibody immobilized on functionalized polypyrrole

S. Chebil[a], I. Hafaiedh[b], H. Sauriat-Dorizon[a], N. Jaffrezic-Renault[b], A. Errachid[b], Z. Ali[c], H. Korri-Youssoufi[a,*]

[a] Equipe de Chimie Bioorganique et Bioinorganique, ICMMO, UMR CNRS 8182, Université Paris-Sud, Bât. 420, 91405 Orsay, France
[b] Laboratoire des Sciences Analytiques, UMR CNRS 5180, Université Claude Bernard-Lyon1, Bat. Raulin, 69622 Villeurbanne Cedex, France
[c] The Teesside Centre for Nanotechnology and Microfabrication (TCNM), University of Teesside, Middlesbrough, UK

ARTICLE INFO

Article history:
Received 19 January 2010
Received in revised form 11 June 2010
Accepted 27 June 2010
Available online 3 July 2010

Keywords:
Deep vein thrombosis
D-dimer
Polypyrroles
Redox marker
ANTA/Cu^{2+}
Electrochemical detection

ABSTRACT

We describe a rapid and sensitive method for detection and quantification of D-dimer which is a biomarker present at elevated concentrations in patients with deep vein thrombosis (DVT) disorders. The method uses an immunosensor based on a single-chain antibody (ScAb) immobilized on a transducer surface and with a densely packed receptor layer. Detection is based on the redox activity of a N-alpha bis(carboxymethyl)-L-lysine (ANTA)/Cu^{2+} complex attached to a polypyrrole backbone. The resulting hybrid material: polypyrrole ANTA/metal complex/His-tag ScAb was characterized by AFM, surface plasmon resonance (SPR) and differential pulse voltammetry (DPV) for the optimization of the biosensor formation. The biosensor offers a promising template for antibody immobilization and for immunodetection of a specific D-dimer. The biosensor shows a remarkable variation in redox activity of the ANTA/Cu^{2+} complex after the D-dimer association with a binding constant K_d of 1 ng mL^{-1}. Electrochemical impedance spectroscopy (EIS) allows monitoring D-dimer association with a linear response between 0.1 ng mL^{-1} and 500 ng mL^{-1} and a detection limit of 100 pg mL^{-1} in PBS is obtained. The biolayer exhibits the same sensitivity for the detection of D-dimer in human patient plasma samples. This assay method is versatile, offers enhanced performance for the evaluation of proteins association and could easily be extended to the detection of other proteins, present in serum human sample.

1. Introduction

Veinous thromboembolism (VTE), comprising deep vein thrombosis (DVT) and pulmonary embolism (PE), is a common disease with reported annual incidences varying roughly from 120 to 180 per 100,000 persons in the USA and Europe (Silverstein et al., 1998; Oger, 2000; Cushman et al., 2004). The diagnosis of VTE is often missed because of the high variability in the clinical symptoms associated with the disease. As a result, the mortality rate of VTE and especially of PE, which is a severe and common complication of DVT, is high (Cushman et al., 2004), and therefore should be suspected in patients presenting even vague symptoms suggestive of VTE. Increasing efforts are presently aimed at establishing earlier and more accurate diagnoses of VTE, which can be reliably, diagnosed using different imaging methods, such as ultrasonography or helical computed tomography (CT) (Srivastava et al., 2004; Zierler, 2004). However, although non-invasive, these imaging techniques remain relatively time-consuming and expensive. Detection of biomarker present in plasma is a good alternative. D-dimer is a marker of endogenous fibrinolysis and thus it can be detected in patients with DVT (Chu, 2004). In fact, several D-dimer analysis assays are presently available, such as enzyme-linked immunosorbent assays (ELISA), whole blood agglutination assays, and latex agglutination assays. ELISA-based assays are the most sensitive in detecting VTE, and are generally considered as the gold standard for D-dimer testing (Ghanima and Sandset, 2007).

Immunosensors with high sensitivity and selectivity are needed for earlier diagnosis of deep vein thrombosis (Goodacre et al., 2006). The development of affinity biosensors for molecular recognition by antibody–antigen interaction has been an area of increasing interest over the past decade, both for biological and chemical analysis purposes (Belluzo et al., 2008). Label-free biosensors are very simple to handle and allow real-time measurements to be made directly (Berggren et al., 2001). Electrochemical methods are attractive because they are amenable to direct electrical readout, are well suited for rapid detection with low-cost instrumentation, and can be miniaturized (Wang, 1999; Pumera et al., 2007; Sadik et al., 2009).

Conducting polymers (CPs) are widely used as transducers for biological interactions. CPs are polyconjugated polymers with an electronic structure giving them intrinsic characteristics such as

* Corresponding author. Tel.: +33 169157440; fax: +33 169157281.
E-mail addresses: hafsa.korri-youssoufi@u-psud.fr, hafsakorri@icmo.u-psud.fr (H. Korri-Youssoufi).

0956-5663/$ – see front matter © 2010 Elsevier B.V. All rights reserved.
doi:10.1016/j.bios.2010.06.048

electrical conductivity, which can be controlled by a doping/dedoping process, low ionization potential, high electron affinity and optical properties. The electronic structure of a conducting polymer is very sensitive to any modification of the backbone conjugation and conformation related to a biological interaction (Tlili et al., 2005). Thus, the success of CPs as transducers relies on their ability to provide a suitable interface for grafting bioreceptors onto micron-sized surfaces (Grosjean et al., 2005; Livache et al., 1998) and, at the same time, convert biological recognition transfer produced by probe/target interactions into an optical (Ho et al., 2005) or electrical signal (Korri-Youssoufi and Yassar, 2001; Li et al., 1999). Among of CPs used in sensing applications, polypyrrole (Ppy) has been studied due to its biocompatibility, high hydrophilic character and high stability in water (Ramanavicius et al., 2006).

The aim of this work is to develop biosensors for monitoring D-dimers via the immobilization of a single-chain antibody derivative from monoclonal D-dimer antibody 3B6 on an electrode surface. For this purpose we have developed a strategy for the immobilization of the single-chain antibody (ScAb) onto conducting polypyrrole using His-tag/M^{2+}/ANTA chemistry (Aravinda et al., 2009). The ANTA/metal complex plays a double role: firstly it controls the immobilization of the ScAb on the polymer and secondly it enhances the redox activity and the conductivity of the polypyrrole layer. The biosensor was constructed using a layer-by-layer chemical approach. A copolymer was deposited on a gold electrode by electrochemical oxidation of a pyrrole bearing an activated ester (pyNHP) and pyrrole (py) amino functionalized nitrilotriacetic acid (ANTA) was subsequently covalently bonded to the polypyrrole by chemical substitution. Next, bivalent metal ions such as Co^{2+}, Ni^{2+} and Cu^{2+} bound to ANTA by a tetravalent chelation interaction, leaving two vacant coordination sites available to the His-tag antibody (His-tag ScAb) (Haddour et al., 2005; Vallina-Garcia et al., 2007; Schmid et al., 1997). The elaboration of the biosensor was monitored using various techniques infrared spectroscopy (FT-IR), SPR, AFM, DPV and EIS. In the following section we will discuss the sensitivity and selectivity of the detection towards D-dimer, as a marker of deep vein thrombosis, which was monitored by DPV and EIS.

2. Experimental

2.1. Reagents

Lithium perchlorate, N-alpha, N-alpha-bis(carboxymethyl)-L-lysine hydrate (ANTA), copper(II) acetate, cobalt(II) acetate, and nickel(II) chloride were purchased from Sigma–Aldrich. Pyrrole was purchased from across and was distilled before use. The pyrrole functionalized in the 3 position with an ethyl ester-N-hydroxyphthalamide (pyNHP) group was synthesized as described previously (Korri-Youssoufi et al., 1997). Buffer solutions of 10 mM phosphate (PBS) at pH 7.4 and 0.2 M acetate (ABS) at pH 4.6 were prepared and stored at 4 °C.

2.2. Fabrication of ScAb conjugated to His-tag

The anti-D-dimer antibody is a recombinant single-chain fragment (ScAb) produced and purified by Haptogen Company from 3B6 antibody, which is an IgG3/Kappa type molecule containing two high affinity binding sites. The monoclonal antibody was derived from an immunized goat by DBDx phage display technology and is expressed as a fragment antibody ScAb with a His-tag for binding.

The first stage in the expression and purification of the antibody required for the cloning of the heavy variable and light variable chains of the antibody from a protein display plasmid into an expression vector that enables the production of soluble proteins. The variable antibody binding domain was excised by restriction digest and cloned into an expression vector that facilitates the fusion of the antibody variable binding domain to a human light variable chain domain (HuCK) for detection and a polyHis-tag for immobilization. The D-dimer antigen material was quantified and checked in ELISA binding test for antibody specificity of ScAB towards D-dimer in the range of 1–10 $\mu g\,mL^{-1}$. The result of ELISA shows that single-chain antibody is specific to only D-dimer and any other reaction was obtained with non-relevant protein.

2.3. Formation of the polypyrrole layer bearing ANTA/M^{2+} and immobilization of His-tag ScAb

The polypyrrole layer is formed in three steps: firstly, electropolymerization on the gold surface, with two monomers, one functionalized pyrrole (pyNHP) bearing a reactive group and pyrrole itself (py) as spacer, leads to the formation of a conductive poly(py-pyNHP) copolymer layer. Several experimental conditions were studied in order to obtain a stable and reproducible copolymer. Thus, electropolymerization was performed at room temperature by applying a potential of 0.9 V/SCE and a charge of 11 $mC\,cm^{-2}$, and using the ratio of 8 mM py to 2 mM pyNHP. The samples were then washed with distilled acetonitrile and dried under argon flow.

ANTA groups were immobilized on polypyrrole by immersing the copolymer layer in a 7 mM of ANTA solution at pH 9 for 1 h. The interaction between the transition metal ions Co^{2+}, Ni^{2+} and Cu^{2+}, and the ANTA was realised using 3.5 mM solutions of copper(II) acetate, cobalt(II) acetate or nickel(II) chloride in acetate buffer (at pH 4.6 for 15 min). His-tag fragment variable single-chain antibody was immobilized by dipping the poly(py-pyANTA/M^{2+}) layer into 8 $\mu g\,mL^{-1}$ His-tag ScAb in PBS for 30 min followed by a blocking step with 50 $mg\,mL^{-1}$ casein solution for 3 min. After each step of biosensor construction, the electrode was washed with PBS, then water. Antibody and antigen was interacted in PBS at pH 7.4 for 30 min at room temperature.

2.4. Instruments

Cyclic voltammetry (CV) was performed with an AUTOLAB" PGSTAT 20 electrochemical analysis system with GPES software. The electrochemical cell comprises three electrodes: a platinum counter-electrode, a saturated calomel reference electrode (SCE) and a circular gold surface as working electrode ($3.14 \times 10^{-2}\,cm^2$).

Electrochemical impedance spectroscopy (EIS) measurements were performed with the Voltalab 80 impedance analyzer in the frequency range 0.05 Hz to 100 kHz, using a modulation voltage of 10 mV. During the measurements the potential was maintained at −1.2 V. The electrochemical impedance experiments were conducted using a conventional three-electrode cell, with a SCE reference electrode, a platinum wire as counter-electrode (0.54 cm^2) and a modified gold working electrode (0.19 cm^2).

FT-IR spectra were measured using a Bruker IFS66 FT-IR spectrometer equipped with a MCT detector and attenuated total reflectance (ATR) with a germanium crystal.

Atomic force microscopy. A commercial dimension 3100 (Vecco instruments, USA) atomic force microscope (AFM) was used for topographical characterization of the samples. All measurements were performed in the tapping™ mode using rectangular silicon AFM tip (MikroMasch NSC18/AIBS) with a spring constant of 3.5 $N\,m^{-1}$ and 75 kHz resonance frequency in air, with relative humidity around 30% and at room temperature.

SPR signals. An AUTOLAB ESPRIT double-channel instrument with an autosampler incorporated was used to perform the optical measurements of the SPR angle. The standard electrochemical cuvette allowed measurements on a three-electrode system con-

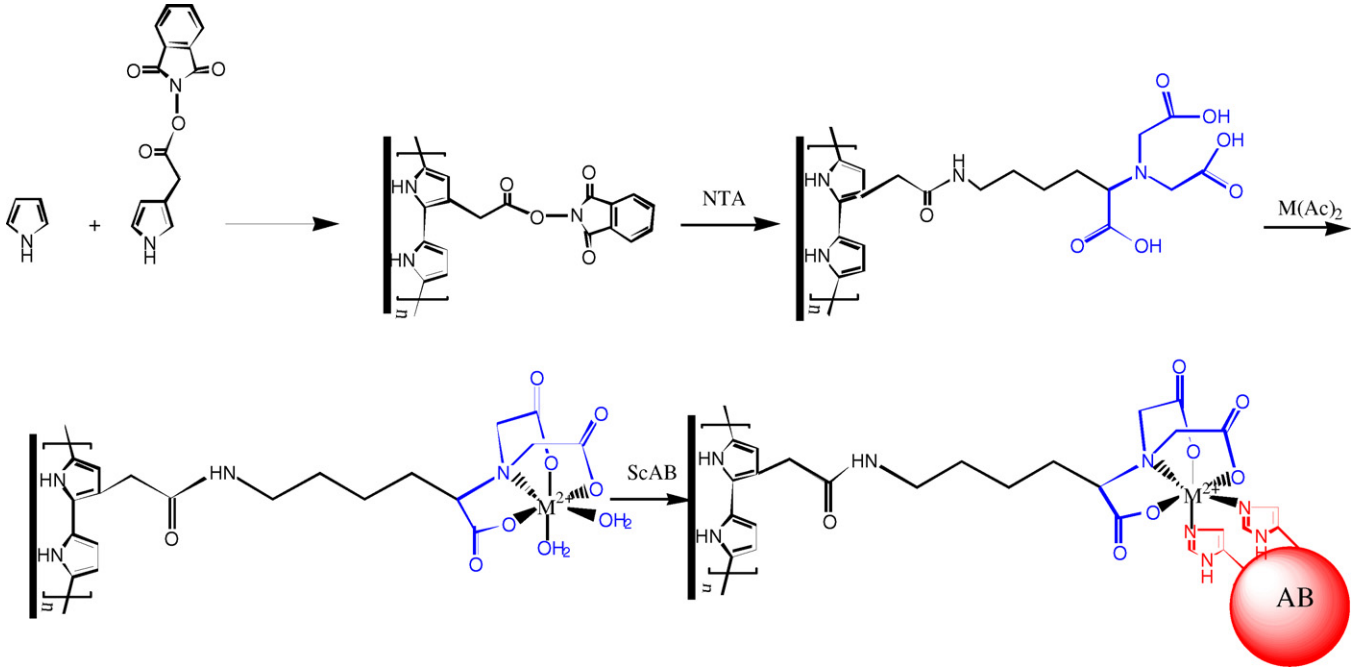

Scheme 1. Description of chemical reactions occurring in the formation of modified polymers.

taining a fixed contact point to the gold layer of the sensor disk acting as working electrode, a replaceable Ag/AgCl reference electrode and a fixed platinum counter-electrode. A normal cuvette is available for SPR measurements where biomolecular interactions are studied.

3. Results and discussion

The conducting biolayer was produced by the electropolymerization of two pyrrole monomers, one bearing an activated ester as precursor (pyNHP) for chemical substitution by ANTA and pyrrole as spacer (py). The conditions of polymerization and the ratio between the two monomers were optimized in order to prevent steric hindrance to the antibody. From these studies a 1:4 ratio of pyNHP to py was selected. The ANTA was then covalently attached to the polypyrrole by reaction of its terminal amine function with the activated ester, leading to the poly(py-pyANTA) copolymer layer (Scheme 1). The complex between ANTA and a metal ion was formed by interaction of the metal salt with the modified polymer in buffer. The interaction of the metal ion with the non-functionalized nitrilotriacetic acid (NTA) ligand is known to form a stable complex, and has been extensively studied and characterized in relation to its use in affinity chromatography for protein purification (Ueda et al., 2003; Khan et al., 2006). Thus, the NTA metal(II) complex is widely used for protein purification due to its high affinity towards donor groups. The NTA complex leaves two coordination sites available for the reversible binding of the peptide sequence histidine unit through two N-imidazoles (Kronina et al., 1999; Bayramoglu et al., 2006). By analogy, His-tag ScAb was immobilized on the poly(py-pyANTA/Cu^{2+}) film by completing the coordination of the Cu^{2+} ion with the two N-imidazoles of the His-tag antibody (Scheme 1).

3.1. Characterization of poly(py-pyANTA/M^{2+}/His-tag ScAb) copolymer

The characterization of the copolypyrrole layer such as the thickness and the molecular structure before and after the covalent attachment of the ANTA and copper interaction was performed by various techniques (see supporting information). We demonstrate that a thin layer (10 nm) of functionalized polypyrrole bearing ANTA and copper is obtained.

The surface topologies of the modified gold surface were imaged using AFM in the contact mode for a 1 μm × 1 μm substrate region. Fig. 1A shows images of the copolymer layer after the different steps in biosensor formation. A roughness parameter was calculated, which gives an indication of the layer density after each step (Cecchet et al., 2007). The poly(py-pyNHP) layer is characterized by a globular morphology at the micrometer scale, as expected for polypyrrole (Dong et al., 2006; Silk et al., 1998) with a roughness factor of 5 nm, which is comparable to the value obtained with polypyrrole functionalized with N-hydroxysuccinimide in nitrogen position poly(pyrrole-NHS) (Ionescu et al., 2007). The covalent grafting of ANTA groups leads to the same structure with a decrease in the calculated roughness factor, estimated to be 3.99 nm. Copper ion interaction with the ANTA carboxylic groups leads to well organized nano-aggregated particles which are still observed after His-tag ScAb immobilization, demonstrating that ScAb has a good organization and orientation on this surface.

The formation of the biolayer was also directly monitored by SPR. The sensorgram (Fig. 1B) shows the variation of the angle versus time following the layer-by-layer formation of the biosensor, ANTA binding, copper interaction and His-tag ScAb association. Each step is followed by a washing step. The kinetic curve corresponding to interaction between the film and the His-tag ScAb shows that this is fast and reaches a plateau after 18 min. The washing step corresponds to the dissociation of the non-anchored His-tag ScAb. The measurement of the angle variation before the interaction and after the washing step can be related to the quantity of antibody anchored on the film (Dong et al., 2008). Using simulation methods (Stenberg et al., 1991) the amount of immobilized ScAb was evaluated at 15 pmol mm^{-2}. Assuming that the His-tag ScAb occupies a surface of 10 nm^2 (Kuby, 1994) the immobilized ScAb on poly(py-pyANTA/Cu^{2+}) forms a highly dense monolayer. This is in agreement with AFM measurements which show a dense surface after antibody immobilization.

The complex formed with copper ions and ANTA reveals two copper redox couples both in solution and on the polypyrrole layer.

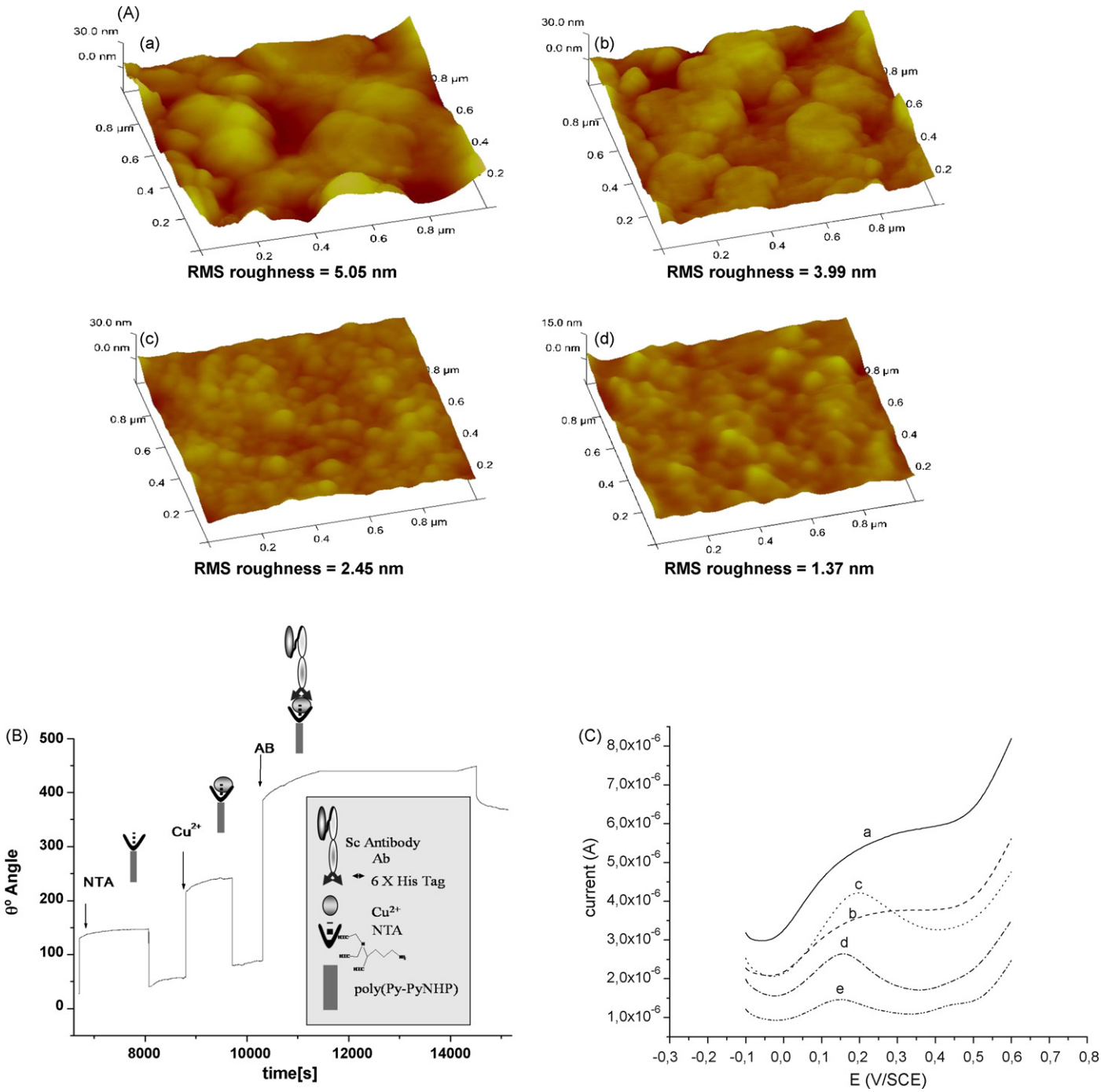

Fig. 1. Characterization of formation of biosensors layer-by-layer (A) AFM images, (B) SPR curves showing kinetic variation and (C) differential pulse voltammetry recorded at a scan rate of 50 mV s^{-1} in 10 mM PBS at pH 7.4 with a pulse height of 45 mV and 0.05 s pulse width; the film is formed on a gold electrode: (a) copolymer poly(py-pyNHP) film; (b) the poly(py-pyANTA) film; (c) copolymer poly(py-pyANTA/Cu^{2+}); (d) copolymer poly(py-pyANTA/Cu^{2+}/ScAb); (e) copolymer poly(py-pyANTA/Cu^{2+}/ScAb) after surface blockage using casein.

A well defined and strong electrochemical signal is obtained in the case of the ANTA/Cu^{2+} complex on the polypyrrole layer. The two redox couples may be attributed to (Cu^{2+}/Cu^{+}) and (Cu^{2+}/Cu^{0}) where the reduction potential at −1.2 V is attributed to the Cu^{2+}/Cu^{0} redox signal and the other, at 150 mV, to Cu^{2+}/Cu^{+}. Unmodified polypyrrole treated with metal ions under the same conditions shows no electrochemical wave at these potentials. Generally, in the case of the ANTA/Cu^{2+} complex deposited on a surface, only an irreversible reduction wave of Cu^{2+} to Cu^{0} is observed at low potential, as shown by the example of ANTA/Cu^{2+} deposited as a monolayer on a carbon electrode (Blankespoor et al., 2005) or on a film of polymerized pyrrole bearing ANTA at the N-position (Haddour et al., 2005). In the present work the observed redox wave of Cu^{2+}/Cu^{+} is the result of a well organized polypyrrole backbone with a high conductivity obtained when it is functionalized after the polymerization step, indicating the ability of the polypyrrole layer to promote easy electron transfer between the copper complex and the electrode surface.

Differential pulse voltammograms were recorded to evaluate the faradaic current of the layers after such steps of biosensor construction. Fig. 1C shows, that the copper (Cu^{2+}/Cu^{+}) redox signal decreases after antibody immobilization, although the potential

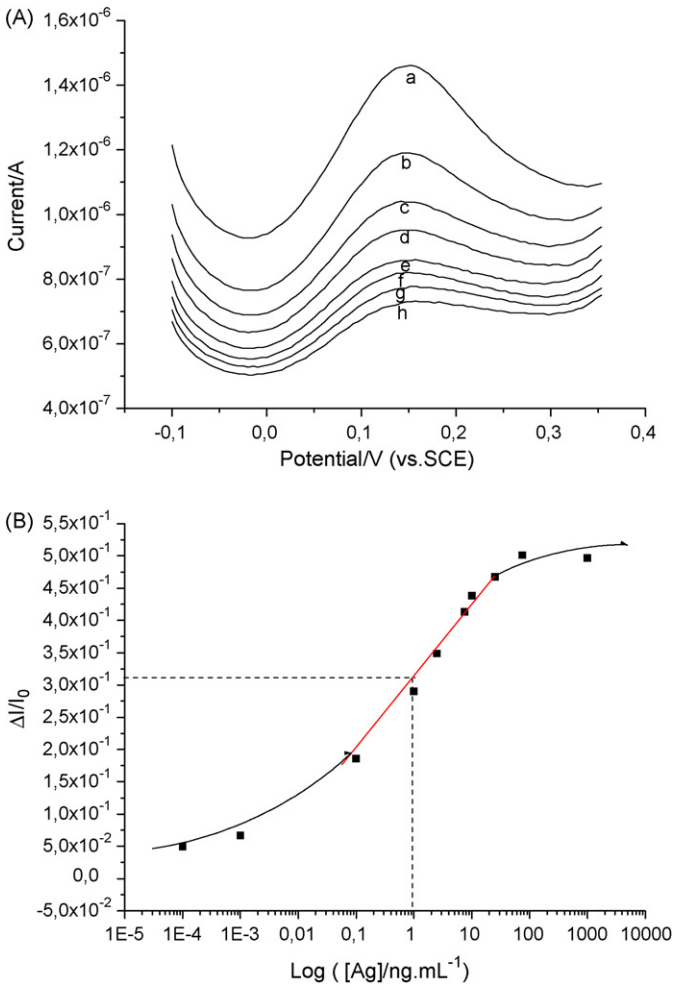

Fig. 2. (A) DPV of poly(py-pyANTA/Cu^{2+}/ScAb) biolayer recorded after antigen interaction between 100 pg mL^{-1} and 0.75 μg mL^{-1}: (a) before antigen interaction, (b) 100 pg mL^{-1}; (c) 1 ng mL^{-1}; (d) 2.5 ng mL^{-1}; (e) 7.5 ng mL^{-1}; (f) 10 ng mL^{-1}; (g) 25 ng mL^{-1}; (h) 75 ng mL^{-1}; DPV are recorded in 10 mM PBS at pH 7.4 at a scan rate of 50 mV s^{-1} with a pulse height of 45 mV and 0.05 s pulse width. (B) Calibration curve obtained by raising the current to a fixed potential of 0.15 V/SCE from DPV curves.

remains unchanged. The immobilization of His-tag ScAb on the ANTA/Cu^{2+} complex leads to a decrease in the current density which can be attributed to the lower electron transfer and mobility of ions due to the size of the antibody. The redox wave decreases after casein immobilization used as blocking agent for interfering compound.

3.2. Electrochemical monitoring of D-dimer detection

The detection of antigen was monitored by differential pulse voltammetry in PBS (pH 7.4) (Fig. 2A). This method allows to measure only the faradaic current, which is generally used for electrochemical detection. The interaction of the immobilized His-tag ScAb on poly(py-pyANTA/M^{2+}) was monitored with several D-dimer concentrations varying between 100 pg mL^{-1} and 10 μg mL^{-1} by successive addition. A decrease in the current density of the oxidation redox signal at 150 mV with an increase in antigen concentration was observed. This proves the higher fixing of D-dimer on the antibody recognition sites induces a large variation in electrochemical signal of the copper anchored on the polypyrrole layer. The decrease in intensity of the copper signal can be attributed to the loss of electrochemical activity of the ANTA/Cu^{2+}/ScAb/Antigen complex due to the blocking effect of the ScAb/Ag interaction. This phenomenon has already been observed in the case of DNA target biosensors obtained with a functionalized redox couple such as a ferrocenyl group on a polypyrrole layer (Korri-Youssoufi and Makrouf, 2001).

The effect of the different D-dimer antigen concentrations on the redox signal of the copper complex was measured by the maximum current value recorded with the potential peak of the redox complex as shown in Fig. 2B. The association constant (K_d) between antibody and antigen was determined by measuring the decrease in the ANTA/Cu^{2+}/ScAb complex redox activity depending on the D-dimer concentration.

The reaction between immobilized antibody and antigen is shown in Eq. (1):

$$\mathrm{Ab} + \mathrm{Ag} \Leftrightarrow \mathrm{Ab{-}Ag}$$

$$K_d = \frac{[\mathrm{Ab{-}Ag}]}{[\mathrm{Ab}][\mathrm{Ag}]} \quad (1)$$

where K_d represents the association constant; [Ab] and [Ag] are the concentrations of ScAb and D-dimer, respectively.

Assuming the ANTA/Cu^{2+}/Ab–Ag produces an inactive complex, the current measured after each addition of antigen is related to the amount of adsorbed Ab–Ag complex formed. The concentration dependences of the adsorbed complex follows the shape of a Langmuir isotherm and can be fitted by the Langmuir equation (2) which allows to calculate the K_d value.

$$\frac{1}{\Delta i} = \frac{1}{\Delta i_{max}} + \frac{1}{K_d\ \Delta i_{max}[\mathrm{Ag}]} \quad (2)$$

where [Ag] is the concentration of D-dimer in solution, K_d is the association constant for the Sc antibody anti D-dimer at a D-dimer binding, Δi is the variation of the current of the ANTA/Cu/Ab–Ag complex and Δi_{max} is the maximum variation obtained corresponding to saturation.

The fitted parameters, estimated by a linear regression of the Hanes–Woolf regression are K_d and Δi_{max}. All errors are reported as 1.0 standard error (SE) at 95% confidence. The calculated K_d value obtained is 1 ng mL^{-1}. Taking into account that the molecular weight of D-dimer is around 180 kDa, the resulting K_d value is 0.5×10^{-11} M. Compared to the value for a monoclonal whole antibody (mAb) III-3b which is reported to bind D-dimer with $K_d = 1.4 \times 10^{-10}$ M (Lugovskoy et al., 2002), the affinity constant is high with the reduced antibody immobilized on this biolayer, where their orientation of the active site of the antibody was optimized for the antigen association.

This result shows that the redox signal of the complex allows to monitor the D-dimer with a sensitivity of 1 ng mL^{-1} and a dynamic range of 1–500 ng mL^{-1}. This result shows the high sensitivity of this system of evaluation of biological recognition with a very wide dynamic range compared to ELISA. Such variation was coming from the immobilization strategy using His-tag ScAb associated directly with redox complex ANTA/Cu^{2+} used as redox probe to follow such association between antibody and D-dimer antigen. The very sensitive redox properties of the complex ANTA/Cu^{2+} to electronic and steric variation in the coordination sphere allows to monitor such association of D-dimer with higher sensitivity than ELISA test.

In order to improve the sensitivity of detection of D-dimer, the interaction with ScAb was monitored by impedance spectroscopy following the variation of the resistive and capacitive properties of the layers after antigen interaction. The impedance $Z(\omega)$ where $\omega = 2\pi f$ with f the signal frequency, is defined as the ratio $U(\omega)$ to $I(\omega)$, where $U(\omega)$ corresponds to the variable ac voltage applied to the electrochemical cell and $I(\omega)$ is the resulting electric current (MacDonald, 2006). This impedance of the biosensor can be represented by an electrical equivalent circuit where at low frequency

the impedance modulus $|Z(f)|$ is proportional to the electron transfer resistance (Huang et al., 2008). The impedance measurements were performed in PBS at potential ranges where the electroactivity of the complex is obtained at −1.2 V/SCE, corresponding to Cu^{2+}/Cu^{0} reduction. The impedance spectra of the biosensor layer at 0.15 V/SCE, where the polypyrrole is in the conducting state and the redox couple of Cu^{2+}/Cu^{+} occurs, indicate diffusion behavior (figure not shown). We demonstrated previously that the impedance recorded at negative potential where the polypyrrole is in a non-conducting state and the charge transfer related to the polypyrrole doping does not take place, allows a low Warburg impedance due to a decrease in ionic movement from the electrolyte to film interface and the diffusion of ions in the film (Hafaid et al., 2009). Thus at negative potential the charge transfer related to the redox signal of Cu^{2+} depends on the level of D-dimer associated to the antibody. The impedance recorded at −1.2 V dc potential in PBS, where the modified electrode with poly(py-pyANTA/M^{2+}/His-tag ScAb) was equilibrated with the specific antigen at concentrations from 0 μg mL^{-1} to 10 μg mL^{-1} is shown in Fig. 3A. The impedance measurement is related to the diffusion of ions from the electrolyte to the electrode surface, the diffusion of ion in the bulk of the film, and the charge transfer of the redox system. The total current through the working interface is the sum of distinct contributions from the faradaic process and double-layer charging.

The formation of the antigen–antibody complex perturbs the doubly charged layer existing at the electrode/electrolyte interface, resulting in an increase in its thickness and the insulation of the electrode surface from the electron transfer of redox system. This results in a capacitance change and electron transfer resistance change, respectively. The high-frequency region is more related to the ionic transfer behaviour, whereas at low frequency the diffusion process becomes the limiting step with the decrease in ac frequency the importance of charge transfer process rises. At low frequency, we observe that the modulus of $|Z(f)|$ increases clearly with the antigen concentration, which indicates that where the antigen is linked to the specific sites of the antibody, the electron transfer resistance increases. To analyze quantitatively the behaviour of biolayers after antigen interaction the experimental results were fitted by the equivalent circuits presented in Fig. 3B. In the circuits, R_S is the so-called high-frequency electrolyte solution resistance, C the double-layer capacitance, R_f the so-called high-frequency ionic charge transfer resistance at the polymer/electrolyte interface and R_h is the low frequency electron transfer resistance of the redox reaction. Antigen immobilization induces an increase in electron transfer resistance of the redox reaction, as generally observed in biolayers after large biomolecule immobilization (Ionescu et al., 2007; Tlili et al., 2008). In order to study the immunosensor response, the calibration curve corresponding to the variation of R_h versus concentrations of specific antigen in PBS, is presented in Fig. 3C. This curve shows saturation at a concentration of 500 ng mL^{-1}. However, the immunosensor exhibits a linear relation with D-dimer concentration ranging from 0.1 ng mL^{-1} to 100 ng mL^{-1} with a threshold of 100 pg mL^{-1}.

3.3. Analytical parameters of the biosensors

The selectivity of the biosensors towards D-dimer compared to other proteins was analyzed with BSA and human IgG. The SPR, DPV and EIS signals were recorded after biosensor formation and after incubation with 1 μg mL^{-1}. The measured signal remains unchanged after incubation with these proteins. Blocking of the polypyrrole layer with casein and the high specificity of the Sc D-dimer antibody prevents non-specific interaction.

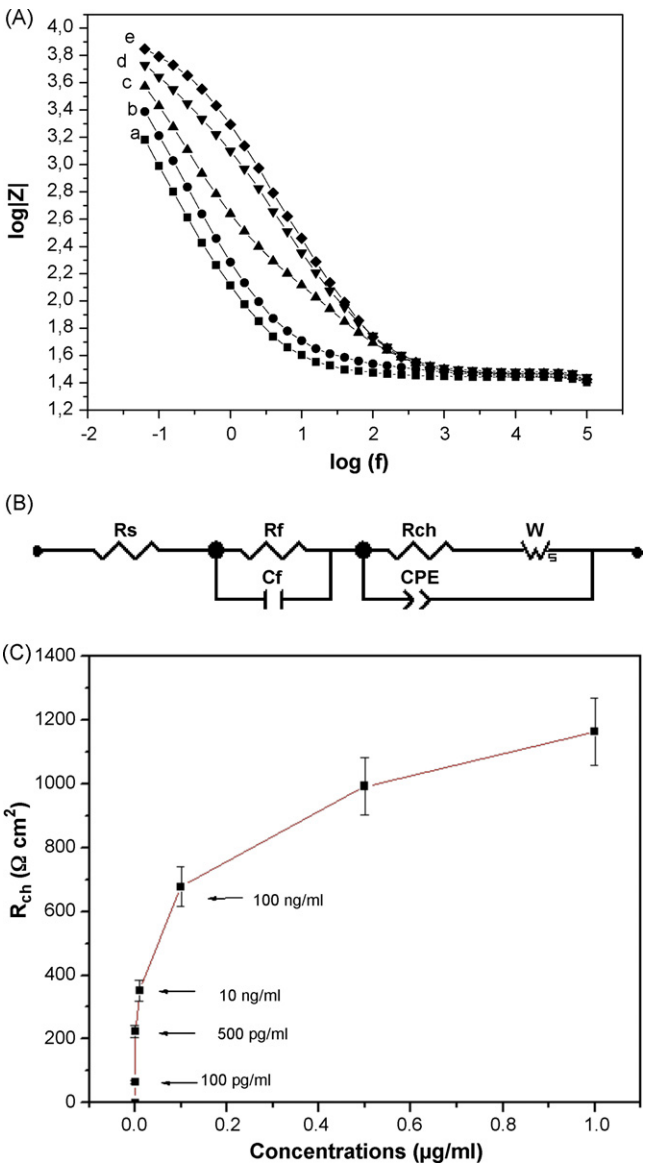

Fig. 3. (A) Bode diagrams related to D-dimer detection at dc potential of −1.2 V/SCE recorded in PBS 10 MHz–100 kHz; amplitude of alternating voltage is 10 mV: (a) before antigen interaction, (b) 100 pg mL^{-1}, (c) 0.5 ng mL^{-1}, (d) 4.5 ng mL^{-1} and (e) 100 ng mL^{-1}. (B) Equivalent circuit fitting and (C) calibration curve obtained of value of the R_{ct} calculated from the circuit fitting.

The reproducibility of the impedance and DPV responses to D-dimer detection was tested on 6 biosensors fabricated by the same procedure; a RSD value of 7% was obtained.

3.4. Electrochemical monitoring of D-dimer detection in plasma sample

The feasibility of the immunoassay system for clinical applications was investigated by analyzing several real samples of human plasma (coming from hospital of Bratislava) with various levels of D-dimer and comparing with the clinical immunoassay PATHFAST which is based on a chemiluminescent enzyme. These serum samples were diluted with PBS at pH 7.0 to different concentrations in the range of 4 ng mL^{-1} to 100 ng mL^{-1} where the biosensor shows the best sensitivity. Table 1 describes the correlation between the results obtained by the proposed immunosensor and the PATHFAST method performed on 4 patients of different ages and sex with various levels of D-dimer. From these data it is clear that there is no

Table 1
Comparison of D-dimer level of plasma samples measured in hospital in patients with DVT and determined with the present biosensor.

Plasma sample	Age and sex	D-Dimer measured in hospital (ng mL^{-1})	Immunosensor (ng mL^{-1})	Relative deviation (%)
1	69 (F)	167	143	14
2	29 (M)	810	793	2
3	64 (F)	900	738	18
4	72 (F)	2500	2250	10

significant difference between the results given by these two methods, indicating that the proposed biosensor could be satisfactorily applied to the clinical determination of D-dimer levels in human plasma.

4. Conclusion

We describe a new procedure for monitoring D-dimer by following the affinity for single-chain D-dimer antibody and using an electrochemical transducer consisting of a highly organized polypyrrole backbone coupled with redox markers ANTA/Cu^{2+} complex. We have shown that this biolayer allows to quantify the association of D-dimer by monitoring the electrochemical properties of the complex. The electrochemical signal of ANTA/Cu^{2+} allows to calculate that the association constant between the Sc D-dimer antibody and the D-dimer is about 1 ng mL^{-1} which demonstrates that reduced antibody has high affinity compared to whole antibody. Impedance spectroscopy shows that the biosensor is able to detect 100 pg mL^{-1} of D-dimer. The biosensors can be applied for the evaluation of D-dimer in human plasma samples with various D-dimer levels. These results underline the remarkable properties of functionalized polypyrrole bearing ANTA/Cu^{2+} complex as redox active sites and selective antibody binding sites for the monitoring the antibody/antigen association. Although this technique has been applied to the specific case of the D-dimer antigen detection, it could be generalized as a platform to follow the evaluation of protein affinity in complement to ELISA method.

Acknowledgment

The authors are grateful for financial support of the European Community Sixth Framework Program through a STREP grant to the DVT-IMP Consortium, Contract No.53086. Haptogen Company is acknowledged by providing the biological materials and Comenius University of Bratislava by providing human plasma samples from patient.

Appendix A. Supplementary data

Supplementary data associated with this article can be found, in the online version, at doi:10.1016/j.bios.2010.06.048.

References

Aravinda, C.L., Cosnier, S., Chen, W., Myunga, N.V., Mulchandani, A., 2009. Biosens. Bioelectron. 24, 1451–1455.
Bayramoglu, G., Ulku Senel, A., Yakup Arica, M., 2006. Sep. Purif. Technol. 50, 229–239.
Belluzo, M.S., Ribone, M.E., Lagier, C.M., 2008. Sensors 8, 1366–1399.
Berggren, C., Bjarnason, B., Johansson, G., 2001. Electroanalysis 13, 173–180.
Blankespoor, R., Limoges, B., Schollhorm, B., Syssa-Magalé, J.-L., Yazidi, D., 2005. Langmuir 21, 3362–3375.
Cecchet, F., Duwez, A.-S., Gabriel, S., Jérôme, C., Jérôme, R., Glinel, K., Demoustier-Champagne, S., Jonas, A.M., Nysten, B., 2007. Anal. Chem. 79, 6488–6495.
Chu, A.J., 2004. Curr. Vasc. Pharmacol. 2, 199–228.
Cushman, M., Tsai, A.W., White, R.H., Heckbert, S.R., Rosamond, W.D., Enright, P., 2004. Am. J. Med. 117, 19–25.
Dong, H., Li, C.M., Chen, W., Zhou, Q., Zeng, Z.X., Luong, J.H.T., 2006. Anal. Chem. 78, 7424–7431.
Dong, H., Cao, X., Li, C., Hu, W., 2008. Biosens. Bioelectron. 23, 1055–1062.
Ghanima, W., Sandset, P.M., 2007. Thromb. Res. 120, 471–476.
Goodacre, S., Sampson, F., Stevenson, M., Wailoo, A., Sutton, A., Thomas, S., Locker, T., Ryan, A., 2006. Health Technol. Assess. 10 (15).
Grosjean, L., Cherif, B., Mercey, E., Roget, A., Levy, Y., Noel Marche, P., Villiers, M.-B., Livache, T., 2005. Anal. Biochem. 347, 193–200.
Haddour, N., Cosnier, S., Gondran, C., 2005. J. Am. Chem. Soc. 127, 5752–6575.
Hafaid, I., Chebil, S., Korri-Youssoufi, H., Bessueille, F., Sassi, Z., Ali, Z., Abdelghani, A., Jaffrezic-Renault, N., 2009. Sens. Actuators B: Chem. 144, 323–331.
Ho, H.A., Doré, K., Boissinot, M., Bergeron, M.G., Tanguay, R.M., Boudreau, D., Leclerc, M., 2005. J. Am. Chem. Soc. 127, 12673–12676.
Huang, Y., Bell, M.C., Suni, I.I., 2008. Anal. Chem. 80, 9157–9916.
Ionescu, R.E., Jaffrezic-Renault, N., Bouffier, L., Gondran, C., Cosnier, S., Pinacho, D.G., Marco, M.-P., Sanchez-Baeza, F.J., Healy, T., Martelet, C., 2007. Biosens. Bioelectron. 23, 549–555.
Khan, F., He, M., Taussig, M.J., 2006. Anal. Chem. 78, 3072–3079.
Korri-Youssoufi, H., Garnier, F., Srivastava, P., Godillot, P., Yassar, A., 1997. J. Am. Chem. Soc. 119, 7388–7389.
Korri-Youssoufi, H., Yassar, A., 2001. Biomacromolecules 2, 58–64.
Korri-Youssoufi, H., Makrouf, B., 2001. Synth. Met. 119, 265–266.
Kronina, V.V., Wirth, H.-J., Hearn, M.T.W., 1999. J. Chromatogr. A 852, 261–272.
Kuby, J., 1994. Immunology, second ed. W.H. Freeman and Company, New York (Chapter 5).
Li, G., Gu, Q., Zhu, J., Zhu, D., Untereker, D.F., 1999. Anal. Lett. 32, 2545–2557.
Livache, T., Bazin, H., Mathias, G., 1998. Clin. Chim. Acta 278, 171–176.
Lugovskoy, E.V., Kolesnikova, I.N., Gritsenko, P.G., Zolotareva, E.N., Gaffney, P., Nieuwenhuizen, W., Komisarenko, S.V., 2002. Thromb. Res. 107, 151–156.
MacDonald, D.D., 2006. Electrochim. Acta 51, 1376–1388.
Oger, E., 2000. Thrombosis 83, 657–660.
Pumera, M., Sanchez, S., Ichinose, I., Tang, J., 2007. Sens. Actuators B: Chem. 123, 1195–1205.
Ramanavicius, A., Ramanaviciene, A., Malinauskas, A., 2006. Electrochim. Acta 51, 6025–6037.
Sadik, O.A., Aluoch, A.O., Zhou, A., 2009. Biosens. Bioelectron. 24, 2749–2765.
Schmid, E.V., Keller, T.A., Dienes, Z., Vogel, H., 1997. Anal. Chem. 68, 1979–1985.
Silk, T., Hong, Q., Tamm, J., Compton, R.G., 1998. Synth. Met. 93, 59–64.
Silverstein, M.D., Heit, J.A., Mohr, D.N., Petterson, T.M., O'Fallon, W.M., Melton, L.J., 1998. Arch. Intern. Med. 158, 585–593.
Srivastava, S.D., Eagleton, M.J., Greenfield, L.J., 2004. Semin. Vasc. Surg. 17, 173–180.
Stenberg, H., Persson, B., Roos, H., Urbaniczky, C., 1991. Colloid Interface Sci. 143, 513–526.
Tlili, C., Korri-Youssoufi, H., Ponsonnet, L., Martelet, C., Jaffrezic-Renault, N., 2005. Talanta 68, 131–137.
Tlili, C., Jaffrezic-Renault, N., Martelet, C.J., Korri-Youssoufi, H., 2008. Mater. Sci. Eng. C 28, 848–854.
Ueda, E.K.M., Gout, P.W., Morganti, L., 2003. J. Chromatogr. A 988, 1–23.
Vallina-Garcia, R., del Mar, M., Suarez, G., Fernandez-Abedul, M.T., Javier Mendez, F., Costa-Garcıa, A., 2007. Biosens. Bioelectron. 23, 210–217.
Wang, J., 1999. Chem. Eur. J., 1681–1685.
Zierler, B.K., 2004. Circulation 109, 14–19.